Heliyon 10 (2024) e26165

Contents lists available at ScienceDirect

Heliyon

journal homepage: www.cell.com/heliyon

Research article

An optimized approach for solar concentrating parabolic dish based on particle swarm optimization-genetic algorithm

Lifang Li [a], Yanlong Zhang [a], Heng Li [a,*], Rongqiang Liu [b], Pengzhen Guo [c,**]

[a] Laboratory for Space Environment and Physical Sciences, Harbin Institute of Technology, Harbin 150001, PR China
[b] State Key Laboratory of Robotics and System, Harbin Institute of Technology, Harbin 150001, PR China
[c] National Key Laboratory of Science and Technology on Tunable Laser, Harbin 150001, PR China

ARTICLE INFO

Keywords:
Solar energy
Compliant parabolic concentrator
Particle swarm optimization-genetic algorithm
Concentrating parabolic dish
Low-cost fabrication

ABSTRACT

Parabolic dish concentrators have demonstrated the highest thermal and optical efficiencies among the available concentrator options. This paper proposes a novel design approach for fabricating large parabolic dish concentrators by employing compliant petals optimized through Particle Swarm Optimization-Genetic Algorithm (PSO-GA). The design concept involves using cables to pull the outer corners of the petals towards the center, resulting in the creation of finely formed dish mirrors. These mirrors are constructed from thin, optimal-shaped metal petals with highly reflective surfaces. In addition, an analytical model is presented to optimize the bending stiffness of the petals by strategically arranging punched holes using PSO-GA. The proposed design concept is validated through the application of Finite Element Analysis and ray tracing software, specifically LightTools, as well as laboratory experiments. Based on the demonstration with a 1m-diameter parabolic dish, it was observed that a receiver surface with a radius of 3.5 cm could achieve an impressive sunlight collection efficiency of up to 98%. This innovative design approach offers several advantages, including simplified fabrication and transportation of flat mirror elements to field sites, which can potentially lead to cost reductions and highly efficient solar energy solutions.

1. Introduction

Parabolic dish concentrators play a vital role in solar energy systems by reflecting solar radiation onto a receiver located at the focal point. They are especially crucial for solar thermal generators, where the concentrators are typically mounted on active tracking systems to follow the sun's movement [1]. At the receiver, a heat engine collects the concentrated sunlight's heat for conversion into electricity or other useable forms of energy. Commonly employed in solar thermal power generation systems are heat engines such as the Stirling and Brayton cycle engines [2–4]. However, the current construction of parabolic dish concentrators relies on conventional structures like metal frameworks, resulting in high costs and bulkiness. These factors limit their practicality and deployment [5–7].

Generally, solar dish concentrators approximate a parabolic shape with multiple, spherically shaped mirrors supported by a truss structure, and other structure accessories are made of steel or aluminum [8]. Examples of these disk-type solar concentrators include the Australian Wizard Power Company and ANU's large-scale Big Dish Solar Concentrator [9], the Louisiana Jet Petroleum Company's

* Corresponding author.
** Corresponding author.
E-mail addresses: 19S108372@stu.hit.edu.cn (H. Li), guopengzhen@hit.edu.cn (P. Guo).

https://doi.org/10.1016/j.heliyon.2024.e26165
Received 23 May 2023; Received in revised form 22 November 2023; Accepted 8 February 2024
Available online 14 February 2024

"Fresnel-like" reflective concentrator (LEC-460) [10], the aluminum foil mirror-based solar collection concept proposed by Bohm Solar Energy Ltd. in the early 1970s, the 7-m diameter parabolic dish concentrator designed and manufactured by Solar Kinetics Inc. for use in Sandia, Albuquerque, the 15.6-m diameter parabolic dish concentrator designed for the "Concentrator-Stirling" joint venture project led by CPG and designed by Wilkinson, Goldberg and Associates (WGA), and the ZED Solar-powered Victus disk concentrator (designed by AEDesign) [2,3,8,11–13]. The use of such materials can also make it difficult to transport and install them efficiently in a cost-effective manner. Therefore, there is a growing need for the development of new and innovative design approaches that can help address these issues and lead to more cost-effective and efficient solar energy solutions.

Numerical investigations have been conducted to facilitate the design of parabolic dish concentrators. For example, Castellanos et al. [14] put forward a mathematical model for a solar dish system, which calculates the appropriate angles and characterizes the solar tracking control system in order to optimize the heat flow. Hafez et al. [15] utilized MATLAB to simulate various designs of parabolic dish Stirling engines, providing theoretical guidance on important factors such as reflector material, reflector shape, receiver diameter, aperture area, focal length, concentration ratio, rim angle, and receiver's aperture area sizing. Ruelas et al. [16] developed a novel mathematical model for estimating the intercept factor of a Scheffler-type solar concentrator, based on the optical behavior and geometry of the concentrator in Cartesian coordinates. Azzouzi et al. [17] devised a heat-equation based model to predict the heat flux and temperature distribution at the focal zone. Pavlović et al. [18] conducted optical and thermal analyses to determine the optimal position of the receiver relative to the concentrator, aiming to maximize optical efficiency and improve the flux distribution on the receiver. Beltrán-Chacon et al. [19] simulated a power generation system comprising a dish concentrator and cavity receiver, proposing a control system that influences mechanical performance through the use of a variable dead volume. It can be observed that the research is primarily focused on optimizing and improving performance parameters of the concentrator and heat flow distribution, with little emphasis on studying how to reduce processing and installation costs.

An alternative option for designing and fabricating a large parabolic dish concentrator is through the use of thin, optimally-shaped flat elastic metal plates with highly reflective surfaces, which can be bent to form an exact parabolic shape, with their shape and thickness optimized based on an analytical model. This design approach avoids conventional metal frameworks, resulting in cost and weight reductions. It also allows for easier transportation and installation, and provides greater flexibility in terms of size and shape customization [5–7,20]. In this approach, the petal is made up of discrete layers to customize the thickness and achieve an exact parabolic shape for fabrication. However, fabrication of larger solar dish concentrators using this approach requires more discrete layers of petal, which is not conducive to efficient fabrication. To address this, new design strategies must be developed that simplify the fabrication process. For instance, optimization techniques such as Particle Swarm Optimization-Genetic Algorithm can be used to determine the optimum spacing and number of layers required for efficient fabrication. This can simplify and streamline fabrication of larger solar dish concentrators, helping to promote more cost-effective and efficient solar energy solutions.

In this paper, we propose an optimized approach for the fabrication of large and compliant solar concentrating parabolic dishes using Particle Swarm Optimization-Genetic Algorithm (PSO-GA). Unlike traditional methods, which rely on the use of layers of petals to adjust the thickness during fabrication, our new approach simplifies the process by equivalentizing the stiffness of a variable-thickness sheet to that of a thick sheet. Our approach involves using Particle Swarm Optimization-Genetic Algorithm to optimize the placement and sizes of holes punched into a variable-thickness sheet. The aim is to achieve an optimal shape for the bending of the sheet into a parabolic form. By punching the holes in specific locations and sizes, we can create the necessary amount of bending stiffness in the sheet to form an exact parabolic shape when it is bent. This new approach eliminates the need for complex layering of

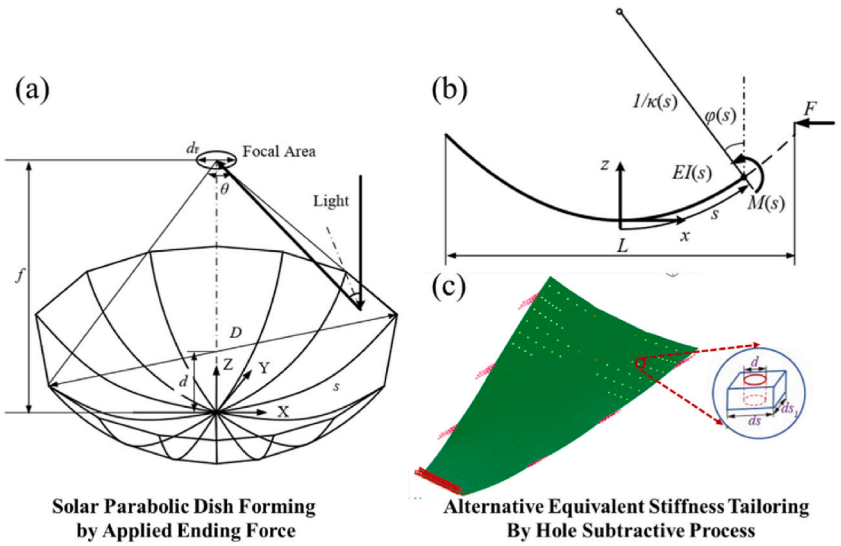

Fig. 1. The scheme for the Parabolic Dish Forming. (a) Solar Parabolic Dish Forming by Applied Ending Force, (b) Petal curvature, and (c) Equivalent Stiffness Tailoring by Hole Subtractive Processing.

petals, simplifying the fabrication process and reducing costs. To validate the effectiveness of our approach, we conducted Finite Element Analysis, utilized ray tracing software-LightTools, and conducted laboratory experiments. These tests confirmed that our concept can effectively simplify the fabrication process of solar concentrating parabolic dishes, resulting in significant cost reductions while maintaining high optical efficiency. A higher optical efficiency implies that more sunlight is effectively gathered at the desired optical focal point. Additionally, this new design approach facilitates easier transportation of flat mirror elements to field sites, further improving the potential for cost reduction and increased optical efficiency in delivering solar energy solutions. This feature is particularly advantageous in space applications where weight and space restrictions are a significant consideration. Thus, the successful validation of our concept highlights its potential for reducing costs and enhancing optical efficiency in delivering solar energy solutions - especially in space applications.

2. Analytical model

2.1. Parabolic shape bending equations based on Euler-Bernoulli beam theory

The parabolic dish concentrator is defined by various parameters and variables. These include the optimal-shaped thin flat metal petals, petal width $b(x)$ and $b(s)$ as functions of x or s respectively, dish diameter D, dish depth d, focal area diameter dF, load force F, focal length f, number of petals N, arc length s, parabolic coordinates x, y, z and rim angle θ. These parameters and variables are shown in Fig. 1(a).

The equation of a paraboloid can be given as:

$$z = \frac{x^2 + y^2}{4f} \tag{1}$$

Assuming Euler-Bernoulli beam theory applies, the deflection of the petals is governed by Ref. [8]:

$$M(s) = EI(s)\frac{\partial \varphi(s)}{\partial s} = EI(s)\kappa(s) \tag{2}$$

In the equation provided, M represents the composite bending moment acting on the end of the parabolic concentrator, while E is the elastic modulus of the material used for the parabolic dish concentrator. I represents the stiffness function of the parabolic dish concentrator and describes its resistance to bending based on the shape and size of its cross-section. Additionally, φ represents the rotation angle of the parabolic trough concentrator, and κ is the curvature of the parabola. These variables are shown in Fig. 1(b).

Here, the curvature of the parabola $\kappa(s)$ is determined by:

$$\kappa(s) = \frac{1}{2f}\left(1 + \left(\ln\frac{s}{2f} + \sqrt{\frac{s^2}{4f^2} + 1}\right)^2\right)^{-\frac{3}{2}} \tag{3}$$

The arc length of a parabola s is defined as follows:

$$s(x) = \int_0^x \sqrt{1 + \left(\frac{u}{2f}\right)^2}\, du \tag{3}$$

where, u is the dummy integration variable along the longitudinal direction.

For a rectangular cross-section, the second moment of area, $I(s)$, can also be given by the following equation:

$$I(s) = \frac{b(s)t(s)^3}{12} \tag{4}$$

where $b(s)$ is the width of the rectangular cross-section, and $t(s)$ is the thickness of the cross-section at an arc length s.

Then, the bending moment $M(s)$ at an arc length s can be expressed as the following Eq. (5), according to Eqs. (1)~(4):

$$M(s) = F\left(h + d - f\ln\left(\frac{s}{2f} + \sqrt{\frac{s^2}{4f^2} + 1}\right)\right) \tag{5}$$

where, F is the force acting on the end of the petal, h is the height from the parabolic dish edge to the force acting point, d is the dish depth, and f is the focal length.

Thus, the petal thickness with petal arc length is thereby governed by:

$$t(s) = \sqrt[3]{\frac{M}{bEk}} = \sqrt[3]{\frac{12F(h + d - x^2/4/f)}{bEk}} \tag{6}$$

Where b is the ideal petal width, and $t(s)$ is the petal thickness with petal length. According to Eq. (6), we can get that a parabolic trough concentrator can be manufactured by varying the thickness of a petal sheet.

2.2. Equivalent Stiffness Tailoring by Hole Subtractive Processing

An alternative method for achieving equivalent stiffness between a variable-thickness sheet and a thick sheet is through holes subtractive processing. This technique can reduce processing difficulty without sacrificing the effective reflective area of the sheet. In the model, assuming the initial equal thickness of the band sheet is t_0, the deviation between the equal thickness and the variable-thickness thin plate can be derived as follows:

$$\Delta t = t_0 - t(s) \tag{7}$$

Then, the relationship between force F and arc length s is governed by a functional $F(s)$, shown as:

$$F(s) = F(\Delta t(s)) \tag{8}$$

By taking the total change of Δt as a reference, the volume replacement method can be employed to remove an equivalent volume of material by punching multiple small cylindrical holes in the petal sheet. This method ensures that the principle of minimum total volume is satisfied. By selecting a suitable force F to perform petal bending and material reduction on the entire compliant petal sheet, an approximate bending effect can be achieved. The Volume-Equal Thickness Transformation can be determined by the following equation:

$$dt * ds * ds_1 = \frac{\pi d^2}{4} * t_0 \tag{9}$$

wherein: dt is the difference between t_0 and $t(s)$; ds and ds_1 are differential calculus in the length and width direction, respectively; d is

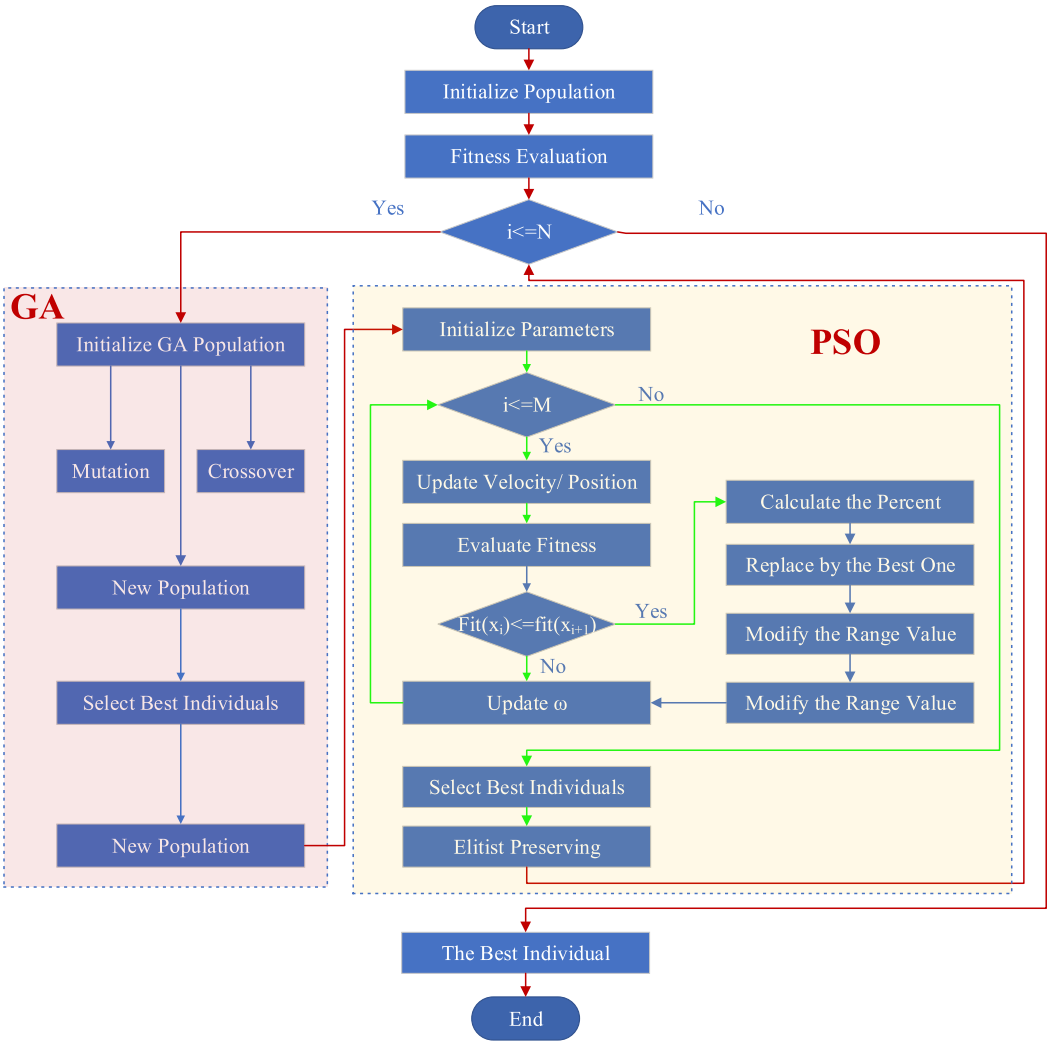

Fig. 2. The Optimization algorithm flowchart for the PSO-GA.

the diameter of the hole; t_0 is the thickness of uniform petal sheet.

2.3. Particle swarm optimization-genetic algorithm

In order to investigate the distribution of punching holes and the impact of end force on the parabolic forming effect, the Particle Swarm Optimization-Genetic Algorithm (PSO-GA) has been employed. By utilizing the memory function of the PSO to store all information on particles, the GA can enable the sharing of information between chromosomes. In turn, this allows the entire population to undergo gradual evolution towards the optimal population, ultimately leading to the discovery of the optimal solution [21,22].

If the fitness value of the population in the m+1 generation aligns more closely with the target than the fitness value of the m generation, the change direction of the entire population in the m+2 generation is determined by its relative change direction to the m generation, using its relative step size as a reference for the search step size. Should the result of the m+2 generation prove to be worse than that of the m + 1 generation, the result is discarded and the search continues with the aid of information sharing between particles in the PSO algorithm.

The findings indicate that during the initial stages of the algorithm, PSO outperformed GA with regards to discovering optimal solutions. However, with an increase in the number of generations, the effectiveness of PSO gradually decreased. Based on the strengths and weaknesses of both algorithms, the PSO-GA algorithm was modified to optimize its performance. The detailed process flowchart can be viewed in Fig. 2. The particle swarm algorithm enables the optimization of both the weighted value w and update speed v. The weighted value w is determined by:

$$w_i(t+1) = \begin{cases} min\left(1, w_i(t) + (1-w_0) \times exp\left(\dfrac{\left(x_i(t+1) - best_i(t)^2\right)}{-2\delta^2}\right) + \varepsilon\right), \\ \qquad if\ \delta_i(t) \geq 0\ and\ \delta_i(t-1) \geq 0 \\ w_{id}(t)\ else \\ max\left(0.1, w_i(t) - w_0 \times \left(1 - exp\left(\dfrac{\left(x_i(t+1) - best_i(t)^2\right)}{-2\delta^2}\right)\right) - \varepsilon\right), \\ \qquad if\ \delta_i(t) < 0\ and\ \delta_i(t-1) < 0 \end{cases} \tag{10}$$

and, $\delta_i(t)$ is defined as follows:

$$\delta_i(t) = \begin{cases} 1\ if\ fit(x_i(t+1)) < fit(best_i(t+1)) \\ -1\ \ else \end{cases} \tag{11}$$

In the process, w_i (t+1) is determined by w in (t+1)-generation; w_0 is the initial given value; x_i (t+1) is the variable of (t+1)-generation; $best_i$ (t+1) is the (t+1)-generation fitness optimum.

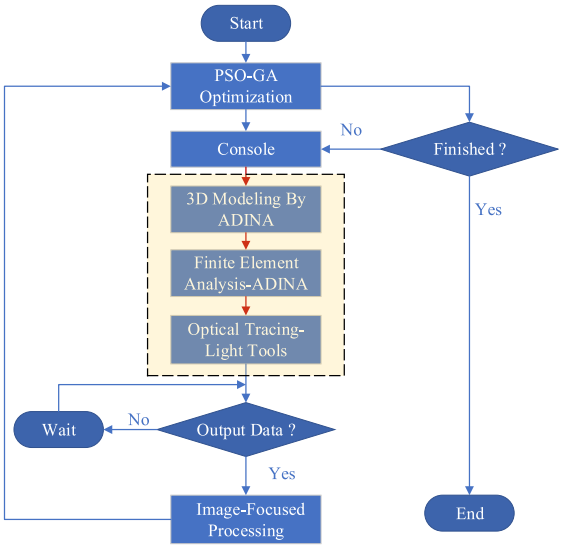

Fig. 3. PSO-GA based optimization strategy for parabolic dish concentrator.

3. Optimization-based verification

3.1. PSO-GA Based Optimization Strategy for Parabolic Dish Concentrator

The study focused on achieving parabolic forming through the lamination of two layers of thin plates. The upper layer was designed to function as a substrate for the reflective film, while the lower layer acted as a supporting rib. By combining the two layers, the entire compliant thin plate was able to bend in a way that created the desired parabolic shape.

In general, it can be challenging to conduct simulation modeling research on nonlinear deformation. Hence, we utilize the advanced nonlinear large deformation analysis function in finite element simulation software to create a robust simulation model that can process and analyze the porous distribution of compliant thin plates. This enables us to investigate the impact of the forming effect of the compliant sheet.

We employed a method involving software interaction, as depicted in Fig. 3, which utilizes the Fourier function to discretize the stiffness of the underlying sheet. By leveraging PSO-GA as the core of the optimization algorithm, we were able to investigate the bending of compliant sheets. To assess the concentrating effect of the entire dish concentrator, the Monte Carlo ray tracing method was employed to conduct optical simulation of the parabolic dish concentrator unit. Focusing spot results were obtained and an evaluation function was established for further analysis.

During the simulation optimization process, optical simulation analysis software enables us to obtain the focused image intuitively and accurately. During this process, focus deviation, the size of the highest temperature region, and the size of other temperature regions are the primary parameters of interest. Based on the quality of the spotlight image, an objective function can be constructed [23].

The concentrated image obtained has been processed using the following method, as shown in Fig. 4:

a) Grayscale transformation enhancement: The image is preprocessed to facilitate the extraction of key area information. Important areas are extracted and separated, then converted into binary images.
b) Image smoothing: Salt and pepper noise and Gaussian filtering technology are applied to further refine the binarized image to an ideal state.
c) Data statistics: The binarized image is separated into a blue area A1 and a red area A2. Statistical analysis is performed on the pixels within each area, and the extracted statistical pixel values are denoted as NB and NR, respectively, using 4-connected area image statistics technology.
d) Extraction of center point data: The extracted NR and statistical functions are used to determine the center position M (x, y).

With the aforementioned image processing method, the blue area A1 and the red area A2 can be separated and the pixels within each region can be statistically analyzed using the connected area method. This leads to the determination of NB and NR for each region. Mathematical expressions can then be constructed to perform further analysis and processing.

The focus deviation can be calculated using the following formula:

$$D_R = \sqrt{(x - x_0)^2 + (y - y_0)^2} \tag{12}$$

The fitness function (F_f) is determined by:

$$F_f = c_1 \frac{N_B}{\max(N_B)} + c_2 \frac{N_R}{\max(N_R)} + c_3 \frac{D_R}{\max(D_R)} + c_4 \eta \tag{13}$$

where, N_B is pixel value in blue area, N_R is pixel value in red area, η is the optical efficiency, and $c_1 \sim c_4$ are the weighting coefficients. Hence, focus radius, focus bias and optical efficiency can be optimized.

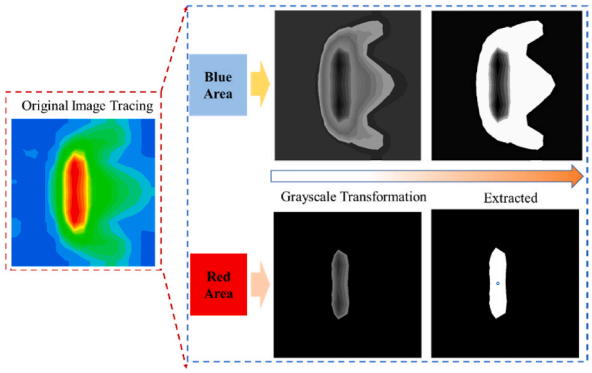

Fig. 4. Extracting the focus image of parabolic dish concentrator by light tracing simulation.

3.2. Optimizing simulation results

A parabolic dish concentrator with a diameter of 1 m and 12 petals has been designed using the practical and cost-effective material 38Si6. The specific parameters are provided in Table 1. The focal length and dish depth of the concentrator are 0.60355 m and 0.10355 m, respectively. Utilizing the PSO-GA based optimization strategy, sunlight can be effectively collected by the absorber, as depicted in Fig. 5.

The study has shown that changes in the distance between the holes during the optimization simulation process had minimal impact on the light-gathering efficiency. However, the size of the holes had a significant effect on the light-gathering efficiency. Larger hole sizes resulted in better light-gathering efficiency. Fig. 5(a) illustrates the distribution of hole sizes and their corresponding light-gathering efficiencies. Remarkably, a hole size of 6 mm had the highest light-gathering efficiency, achieving 89% (nearly 90%). It is important to note that if the hole size exceeds a certain limit, it can cause the petal to break during the bending process. Consequently, a hole size of 6 mm was ultimately selected in the final optimization process to avoid risking petal breakage.

Fig. 5(b) shows the subtractive holes model established using Adina software. The problem assumes large deformation and small strain, with no plastic deformation, only elastic deformation. For accurate simulation of the actual process, bending angle and displacement boundary conditions are applied to the model. Discrete points are used to establish elements one by one, forming the entire shape of the rib. The Gluemsh function is then used to combine the two shell elements for calculation, thereby simulating the laminated structure in the actual process.

The model in LightTools is depicted in Fig. 5(a) (inset Figure), and the model derived from the finite element results has been simulated using the Monte Carlo method. Constraints and objective conditions have been determined by:

$$\begin{cases} min\ F_f \\ s.t.\ min(displacement_i) < displacement_i < max(displacement_i) \\ s.t.min(y_i) < width_i < max(y_i)\ \ i = 1, 2, \ldots m \\ s.t.min(moment_i) < moment_i < max(moment_i)\ \ i = 1, 2, \ldots m \\ s.t.min(\mathrm{height}_i) < h\mathrm{eight}_i < max(h\mathrm{eight}_i)\ \ i = 1, 2, \ldots m \end{cases} \tag{13}$$

where, *displacement* is the boundary condition, *y* is the width, *moment* is the torque, and $height_i$ is the position of the absorber.

Fig. 5(c) illustrates the optimal petal's light-collecting ability, which achieves an almost 90% focus efficiency consistent with the entire parabolic dish concentrator demonstrated in Fig. 5(d). The light-focusing radius is 32 mm, resulting in an impressive concentration ratio of up to 270. Typically, dish concentrators' total concentrating efficiency falls below 95%, making the 90% concentration efficiency realized in this study a viable option for practical applications [1,5,11,12,24].

4. Experimental Verification

We conducted a case study to verify the effectiveness of the optimal approach mentioned earlier in this study. During our experiment, we assembled the concentrator unit using a perforated surface support panel, a shape-optimized support rib, and a 0.1 mm-thick aluminum-coated reflective film, all shown in Fig. 6(a). The assembly process followed a specific method: first, we cleaned the surface of the support panel, then attached the aluminized reflective film using its back glue, and finally riveted the support panel, reflective film, and support ribs together. The resulting prototype in Fig. 6(b) has a diameter of 1000 mm and a height of 800 mm. The compliant parabolic dish concentrator is constructed using a pull rope mechanism in the center, allowing the unit to be transformed from a flat plate to a parabolic shape as required.

Following the creation of the principle prototype, we conducted a theoretical verification of the compliant parabolic mirror unit by subjecting it to sunlight and analyzing the actual effect. Based on the theoretical model, a receiver surface with a radius of 3.2 cm was expected to collect nearly 90% of the sunlight, whereas the actual concentration effect demonstrated that a receiver surface with a slightly larger radius of 3.5 cm could collect as much as 98% of the sunlight. The excellent concentration performance of the mirror unit was thereby confirmed, as evidenced in Fig. 6.

Table 1
Designed dish Parameters.

Parameters	Value
Diameter D (m)	1
Rim Angle θ (degree)	10
Focal Length f (m)	0.60355
Dish Depth d (m)	0.10355
Number of Petals (N)	12
Material	38Si6
Young's Modulus E (Gpa)	210
Poisson's Ratio	0.30
Petal Sheet Thickness t_0 (mm)	0.5
Rib Thickness t_1 (mm)	0.6

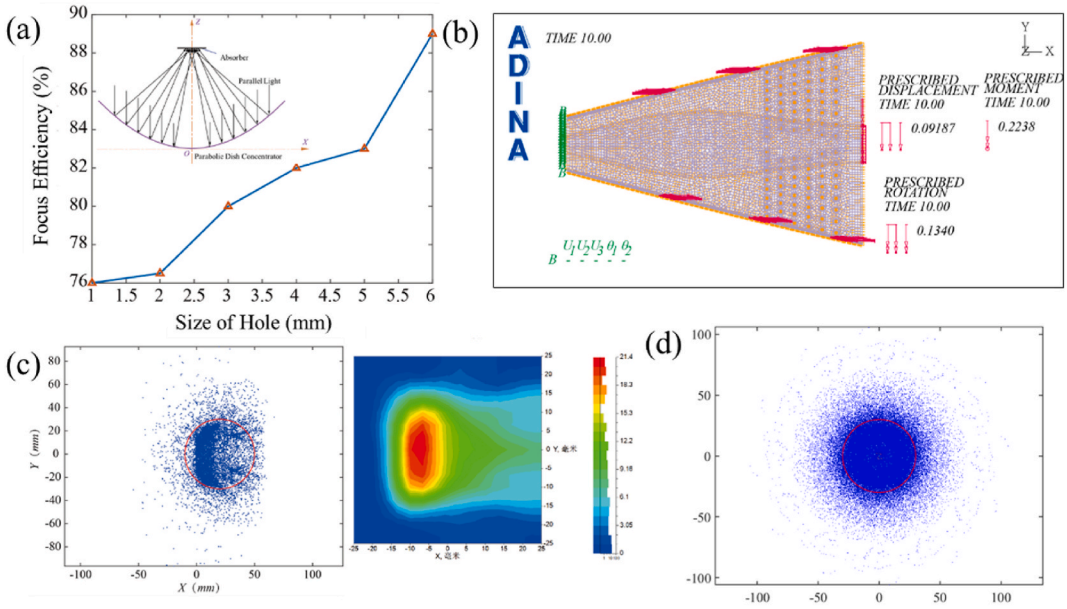

Fig. 5. PSO-GA Based Optimization Verification for Parabolic Dish Concentrator. (a) Curve of Focus Efficiency varying with size of Hole Subtractive Processing, (b) FEA model established with size of 6 mm hole, (c) Light tracing results for the petal, and (d) is the Light tracing result for the whole Dish.

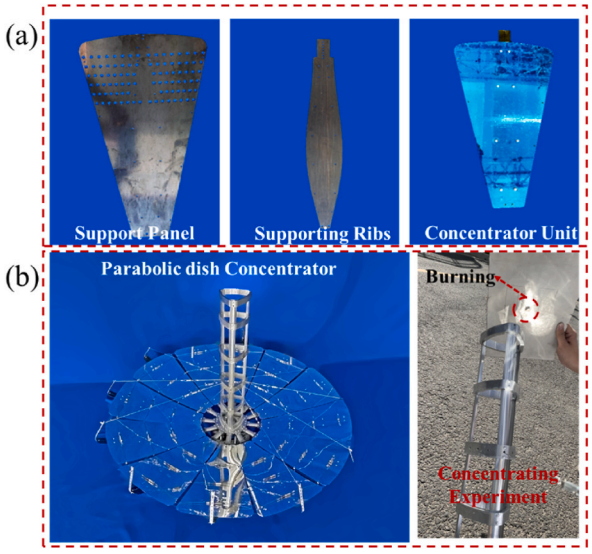

Fig. 6. Experimental Verification. (a) The images of supporting panel, ribs, as well as the concentrator unit fabricated, (b) a case of dish fabricated with concentrating experiment.

5. Conclusion

In conclusion, this paper presents an optimized approach for the fabrication of large and compliant solar concentrating parabolic dishes using PSO-GA. The proposed approach offers the flexibility to customize petal thickness during the fabrication process. By utilizing cables or rods to pull the outer corners towards the center, finely formed dish mirrors can be achieved using optimal-shaped, thin flat metal petals with highly reflective surfaces. An analytical model is introduced in this study, employing PSO-GA to optimize the bending stiffness of the petals through a strategically arranged pattern of punched holes. Through extensive analysis using Finite Element Analysis, ray tracing software (LightTools), and laboratory experiments, the concentration ratio was determined to reach up to 270. One of the key advantages of this concept is the ease of fabrication and shipping of flat mirror elements to field sites. This aspect holds the potential for significant cost reductions and the realization of highly efficient solar energy solutions.

Data availability statement

Data related to this study has not been deposited in a publicly available repository, but will be available upon request.

CRediT authorship contribution statement

Lifang Li: Conceptualization, Funding acquisition, Methodology, Project administration, Supervision. **Yanlong Zhang:** Resources, Writing – review & editing. **Heng Li:** Data curation, Formal analysis, Investigation, Methodology, Resources, Software, Validation, Visualization, Writing – original draft. **Rongqiang Liu:** Supervision. **Pengzhen Guo:** Data curation, Formal analysis, Funding acquisition, Project administration, Resources, Visualization, Writing – original draft, Writing – review & editing.

Declaration of competing interest

The authors declare the following financial interests/personal relationships which may be considered as potential competing interests: Lifang Li reports financial support was provided by National Natural Science Foundation of China.

Acknowledgement

This paper is financially supported by National Natural Science Foundation of China (Grant No. 52275241 and 51835002) and Natural Science Foundation of Heilongjiang Province of China (Grant No. HSF20200042).

References

[1] K. Lovegrove, G. Burgess, J. Pye, A new 500m2 paraboloidal dish solar concentrator, Sol. Energy 85 (2011) 620–626.
[2] K.H. Kumar, A.M. Daabo, M.K. Karmakar, H. Hirani, Solar parabolic dish collector for concentrated solar thermal systems: a review and recommendations, Environ. Sci. Pollut. Res. (2022).
[3] E. Gholamalizadeh, J.D. Chung, Design of the collector of a solar dish-stirling system: a case study, IEEE Access 5 (2017) 20754–20762.
[4] D. Kumar, M. Agrawal, A review on development and applications of solar dish stirling system, in: P. Verma, O.D. Samuel, T.N. Verma, G. Dwivedi (Eds.), Advancement in Materials, Manufacturing and Energy Engineering, vol. II, Springer Singapore, Singapore, 2022, pp. 57–70.
[5] L. Li, S. Dubowsky, A new design approach for solar concentrating parabolic dish based on optimized flexible petals, Mech. Mach. Theor. 46 (2011) 1536–1548.
[6] L. Li, A. Kecskemethy, A.F.M. Arif, S. Dubowsky, Optimized bands: a new design concept for concentrating solar parabolic mirrors, J. Sol. Energy Eng. 133 (2011).
[7] Z. Qiu, P. Li, C. Li, Q. Zhu, T. Zhang, C. Wang, A novel design concept for a reflector of parabolic trough concentrator based on pure bending and correction principle, Sol. Energy 141 (2017) 59–69.
[8] M. Mutyalarao, D. Bharathi, B.N. Rao, Large deflections of a cantilever beam under an inclined end load, Appl. Math. Comput. 217 (2010) 3607–3613.
[9] J. Coventry, C. Andraka, Dish systems for CSP, Sol. Energy 152 (2017) 140–170.
[10] A. Bharti, A. Mishra, B. Paul, Thermal performance analysis of small-sized solar parabolic trough collector using secondary reflectors, Int. J. Sustain. Energy 38 (2019) 1002–1022.
[11] M.Z. Malik, P.H. Shaikh, S. Zhang, A.A. Lashari, Z.H. Leghari, M.H. Baloch, Z.A. Memon, C. Caiming, A review on design parameters and specifications of parabolic solar dish Stirling systems and their applications, Energy Rep. 8 (2022) 4128–4154.
[12] N. Abed, I. Afgan, An extensive review of various technologies for enhancing the thermal and optical performances of parabolic trough collectors, Int. J. Energy Res. 44 (2020) 5117–5164.
[13] R. Verduci, V. Romano, G. Brunetti, N. Yaghoobi Nia, A. Di Carlo, G. D'Angelo, C. Ciminelli, Solar energy in space applications: review and technology perspectives, Adv. Energy Mater. 12 (2022) 2200125.
[14] L.S. Mendoza Castellanos, G.E. Carrillo Caballero, V.R. Melian Cobas, E.E. Silva Lora, A.M. Martinez Reyes, Mathematical modeling of the geometrical sizing and thermal performance of a Dish/Stirling system for power generation, Renew. Energy 107 (2017) 23–35.
[15] A.Z. Hafez, A. Soliman, K.A. El-Metwally, I.M. Ismail, Solar parabolic dish Stirling engine system design, simulation, and thermal analysis, Energy Convers. Manag. 126 (2016) 60–75.
[16] J. Ruelas, N. Velázquez, J. Cerezo, A mathematical model to develop a Scheffler-type solar concentrator coupled with a Stirling engine, Appl. Energy 101 (2013) 253–260.
[17] D. Azzouzi, B. Boumeddane, A. Abene, N. Said, Experimental and parametric study of a solar paraboloid designed to receive a Stirling engine, Mech. Ind. 16 (2015) 206.
[18] S. Pavlovic, E. Bellos, V. Stefanovic, C. Tzivanidis, Z. Stamenkovic, Design, simulation and optimization of a solar dish collector with spiral-coil thermal absorber, Therm. Sci. 20 (2016) 1387–1397.
[19] R. Beltrán-Chacon, D. Leal-Chavez, D. Sauceda, M. Pellegrini-Cervantes, M. Borunda, Design and analysis of a dead volume control for a solar Stirling engine with induction generator, Energy 93 (2015) 2593–2603.
[20] L. Meng, Z. You, A.F.M. Arif, S. Dubowsky, Shape optimized heliostats using a tailored stiffness approach, J. Sol. Energy Eng. 136 (2013).
[21] T. Naheed, I. Usman, T.M. Khan, A.H. Dar, M.F. Shafique, Intelligent reversible watermarking technique in medical images using GA and PSO, Optik 125 (2014) 2515–2525.
[22] H. Liu, R. Zhai, J. Fu, Y. Wang, Y. Yang, Optimization study of thermal-storage PV-CSP integrated system based on GA-PSO algorithm, Sol. Energy 184 (2019) 391–409.
[23] B. Tyler, Interpretation of TOF-SIMS images: multivariate and univariate approaches to image de-noising, image segmentation and compound identification, Appl. Surf. Sci. (2003) 203–204.
[24] A.Z. Hafez, A. Soliman, K.A. El-Metwally, I.M. Ismail, Design analysis factors and specifications of solar dish technologies for different systems and applications, Renew. Sustain. Energy Rev. 67 (2017) 1019–1036.